Supplementary Information

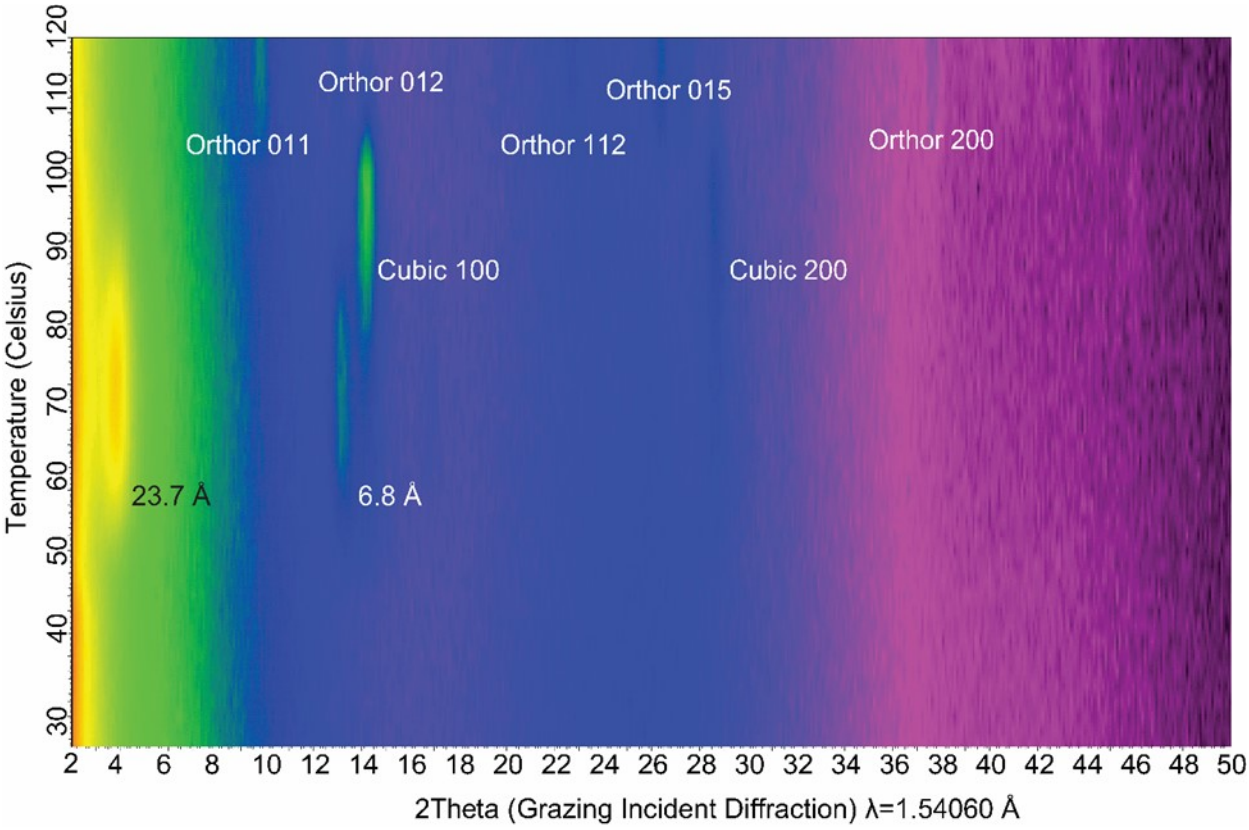

Figure S1: In-situ Grazing Incident XRD studies of 2D perovskite crystals as a function of temperature were used to optimize synthesis conditions.

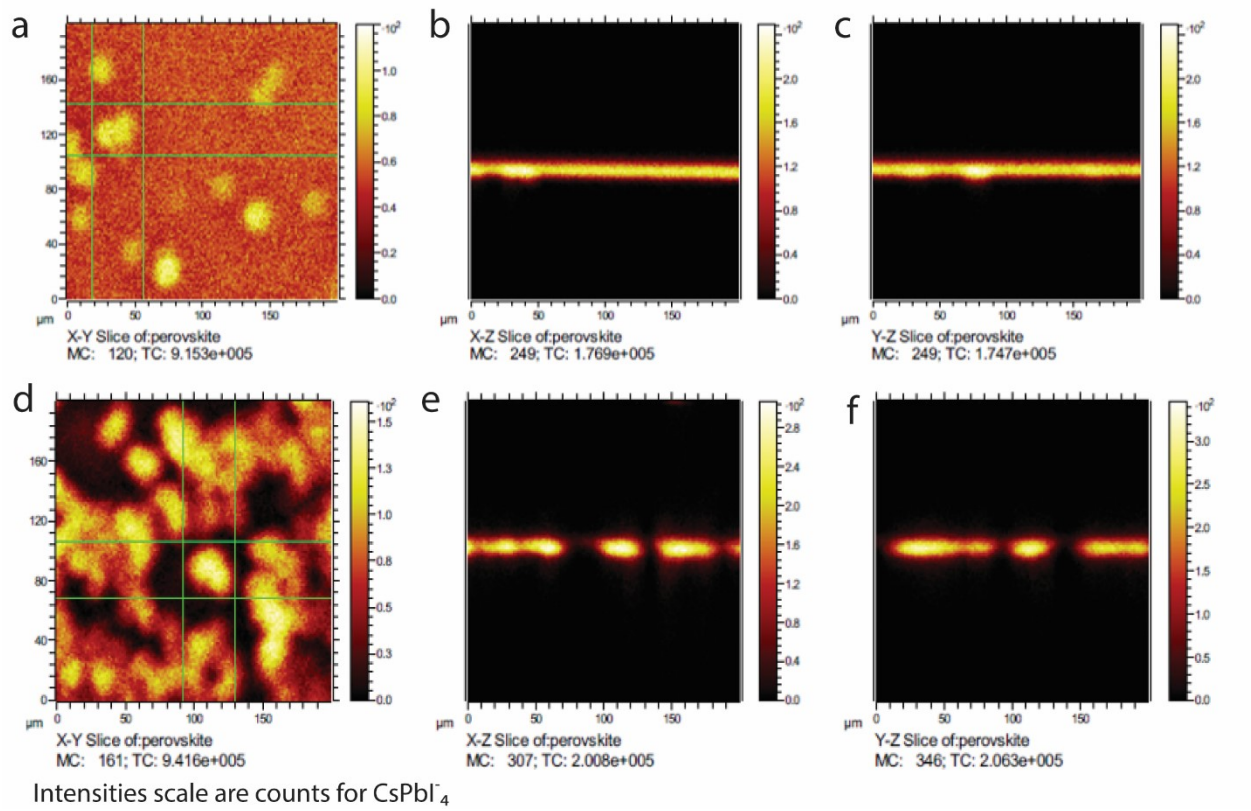

Figure S2: 2D ToF-SIMS images of the combined intensities of ions characteristic of $CsPbI_4^-$ ions within a damaged PSK_CD device. (a) Intensity across the XY plane (defined as parallel to the layers of the device). (b) Images of XZ and YZ slice through the regions defined by the green lines in (a). (d-f) Images of the same ion intensities in the XY plane and an XZ slice of an undamaged PSK_CD device.

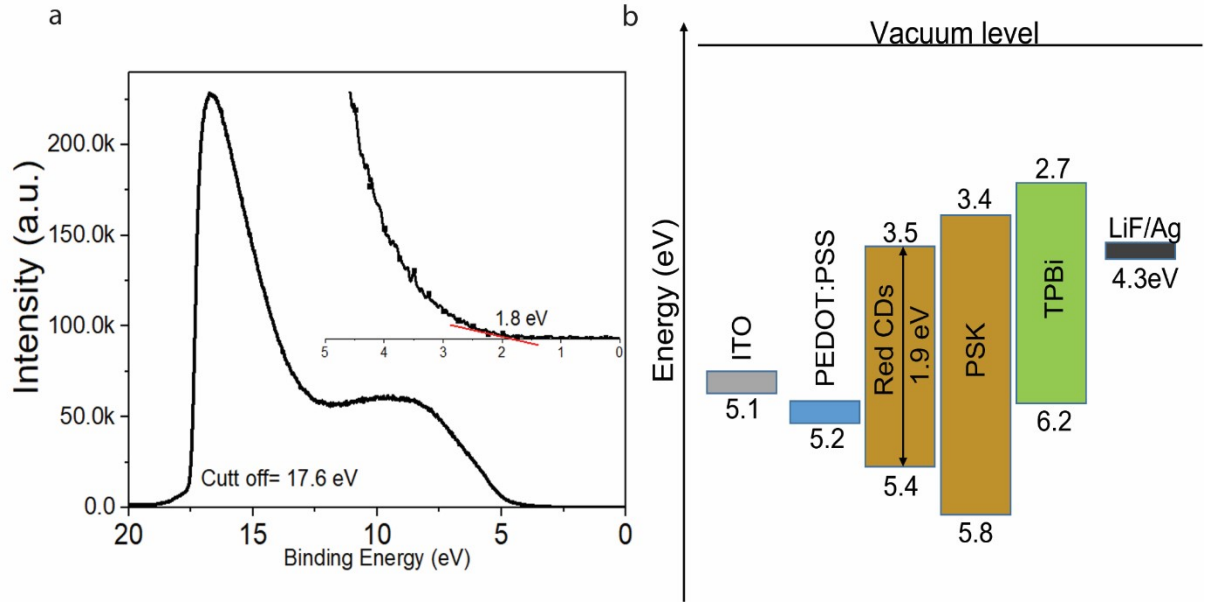

Figure S3: (a) UPS data of red CDs. (b) energy band diagram of the device.

Fabrication of LED: LED devices using PSK and CD-PSK as the active light-emitting layer was fabricated using pre-patterned ITO (Xianyan Technology) deposited glass substrates. The pre-fabrication step involves repeated washing of ITO substrates with Alconox and deionized water. The ITO substrates were rinsed several times in deionized water before ultra-sonicating them in acetone, ethanol, and isopropanol consecutively for 10 minutes each. The ITO substrates were blow-dried with compressed air before spin-coating PEDOT: PSS (Heraeus). PEDOT: PSS was filtered by a 0.45 μm PVDF filter, before spin coating at 5000 rpm for 30 seconds using a spin coater (Laurell Technologies). The spin-coated PEDOT: PSS film was removed from contact pads and then annealed at 150 ^{0}C for 15 mins, before transferring to a glove box system with low moisture and oxygen (O_2 < 0.1 ppm, H_2O < 0.1 ppm). The emitter layers (PSK and CD-PSK) solutions were prepared as discussed in the manuscript's main section. Upon deposition of the emitter layer with a Specialty Coating Systems spin coater, it was then further annealed at 60°C. After emitting layer deposition, samples were transferred to another glove box fitted with a torpedo thermal evaporator, without breaking the vacuum. The 50 nm of 2,2',2"-(1,3,5-Benzinetriyl)-tris(1-phenyl-1-H-benzimidazole [TBPi] (Ossila), 2 nm of lithium fluoride [LiF] (Sigma Aldrich), and 100 nm of silver [Ag] (Sigma Aldrich) layers were thermally deposited consequently at pressures ~10^{-6} mbar. Each substrate consists of six pixels having an area of each device around 10 mm^2.

Instrumentation

Transmission Electron Microscopy (TEM) images of CDs were obtained with a JEOL 2100 TEM, operated at an accelerating voltage of 200 kV.

The Absorption spectrum of the sample was recorded using Cary 60 G6860A spectrophotometer (Agilent).

X-ray Photoelectron Spectroscopy (XPS) experiments were performed on Axis Supra (Kratos) with aluminum Al Ka (hV = 1486.7 eV). All the samples were deposited on glass/ITO, which is grounded with carbon tape for preventing charging during the experiment. Charge compensation was also used, to record the data from each sample. A Kratos AXIS Supra photoelectron spectrometer (He I radiation, hν = 21.22 eV) was used to measure **UPS** energy state of the material.

Time-of-Flight Secondary-Ion Mass Spectrometry (ToF-SIMS) images were acquired using an IONTOF M6 instrument (IONTOF GmbH, Germany) equipped with a reflectron time-of-flight mass analyser, 30 kV Bi/Mn primary-ion source, and argon gas-cluster ion sputter source. Bi_3^+ cluster ions were selected from the pulsed primary-ion beam for the analysis (target current 0.14 pA) and 'bunched' to attain optimal mass resolution ($\Delta m/m > 9000$ for peaks corresponding to the $C_{10\text{-}15}^-$ ions). 3D images of the distribution of ions within the LED devices were obtained by rastering the primary-ion beam across a 200 µm × 200 µm region (at 128 px × 128 px) while sputtering a 500 µm × 500 µm area, centred at the same location, with 10 keV Ar_{1000}^+ ions (target current 10 nA). The pressure in the analysis chamber during data acquisition was 2×10^{-9} mbar.

Photoluminescence Spectra of excitation and emission of both materials were recorded on Fluorescence Spectrophotometer Eclipse G9800A (Cary).

Current-Voltage-Luminance (IVL) Characteristics of devices were recorded using a source meter (B2901A, Keysight Technologies) and a luminance meter (CS-200, Konica Minolta). The electro-luminescence spectra of OLEDs were recorded using a spectrometer (USB 4000, Ocean Optics).

In-situ X-ray Diffraction – Phase Transformation during Heating

The crystal structure changes of the mixture described above during heating were monitored by in-situ XRD using a Rigaku SmartLab Diffractometer equipped with CuKα radiation (λ = 1.5419 Å). The prepared solvent spin-coated on a glass slide was heated in a Rigaku Reactor-X chamber from 26 °C to 200 °C. The sample was scanned isothermally for every 2 °C in Grazing Incident Diffraction geometry at 0.5° incident angle from 2 °2θ to 50 °2θ at a step size of 0.02 °2θ for 20 mins. A parabolic parallel mirror in the CBO module and a 0.228° Post Scattering Analyzer Soller in front of the Hypix3000 detector working in 0D mode were used to define the parallel beam resolution. The measured patterns of different temperatures were aligned in a 2D plot in DIFFRAC.EVA v6 allows the visualization of the phase evolutions as temperature increases.

Pole figure measurement of the synthesized 2D structure

The pole figure of the *001* reflection was measured using a Bruker D8 Advance diffractometer under CoKα radiation (λ = 1.7889 Å). A point focus beam of a 1 mm diameter cross-section was used on the primary side. A 0.3° equatorial soller was used in front of the LynxEye XE-T detector working in 0D mode. The sample was sealed in a semispherical doom holder in an Ar gas atmospheric glove box to avoid any reaction with moisture in the air. The holder was mounted on a Compact Cradle Plus to position 198 orientations on the upper sample hemisphere (χ from 0° to 80°, φ 360°) into the scattering vector direction in the goniometer plane. The intensity of 001 reflection of the PSK structure was measured from 6° 2θ to 9° 2θ at step size 0.05° 2θ. The data was processed in DIFFRAC.TEXTURE software to generate the *001*-pole figure of the PSK phase. Thin-film absorption correction was applied on the pole figure based on 50 nm film thickness and linear absorption coefficient of 1400 cm^{-1}.